



1 Global tropospheric effects of aromatic chemistry with the SAPRC-11
2 mechanism implemented in GEOS-Chem

3 Yingying Yan^{1,2}, David Cabrera-Perez³, Jintai Lin², Andrea Pozzer³, Lu Hu⁴, Dylan B. Millet⁵,
4 William C. Porter⁶, Jos Lelieveld³

5 ¹ Department of Atmospheric Sciences, School of Environmental Studies, China University of
6 Geosciences (Wuhan), 430074, Wuhan, China

7 ² Laboratory for Climate and Ocean-Atmosphere Studies, Department of Atmospheric and
8 Oceanic Sciences, School of Physics, Peking University, Beijing 100871, China

9 ³ Max-Planck-Institute for Chemistry, Atmospheric Chemistry Department, Mainz, Germany

10 ⁴ School of Engineering and Applied Sciences, Harvard University, Cambridge, MA 02138, USA

11 ⁵ Department of Soil, Water, and Climate, University of Minnesota, St. Paul, MN, USA

12 ⁶ Department of Civil and Environmental Engineering, Massachusetts Institute of Technology, 77
13 Massachusetts Avenue, Cambridge, MA 02139-4307, USA

14 Correspondance : Jintai Lin, linjt@pku.edu.cn

15 **Abstract**

16 The GEOS-Chem model has been updated with the SAPRC-11 aromatics chemical mechanism,
17 with the purpose of evaluating global and regional effects of the most abundant aromatics
18 (benzene, toluene, xylenes) on the chemical species important for tropospheric oxidation
19 capacity. The model evaluation based on surface and aircraft observations indicates good
20 agreement for aromatics and ozone. A comparison between scenarios in GEOS-Chem with
21 simplified aromatic chemistry (as in the standard setup, with no ozone formation from related
22 peroxy radicals or recycling of NO_x) and with the SAPRC-11 scheme reveals relatively slight
23 changes in ozone, hydroxyl radical, and nitrogen oxides on a global mean basis (1–4%), although
24 remarkable regional differences (5–20%) exist near the source regions. NO_x decreases over the
25 source regions and increases in the remote troposphere, due mainly to more efficient transport of
26 peroxyacetyl nitrate (PAN), which is increased with the SAPRC aromatic chemistry. Model
27 ozone mixing ratios with the updated aromatic chemistry increase by up to 5 ppb (more than
28 10%), especially in industrially polluted regions. The ozone change is partly due to the direct
29 influence of aromatic oxidation products on ozone production rates, and in part to the altered
30 spatial distribution of NO_x that enhances the tropospheric ozone production efficiency. Improved
31 representation of aromatics is important to simulate the tropospheric oxidation.

32 **1. Introduction**



1 Non-methane volatile organic compounds (NMVOCs) play important roles in the tropospheric
2 chemistry, especially in ozone production (Atkinson, 2000; Seinfeld and Pandis, 2012). Aromatic
3 hydrocarbons such as benzene (C₆H₆), toluene (C₇H₈) and xylenes (C₈H₁₀) make up a large
4 fraction of NMVOCs (Ran et al., 2009; Guo et al., 2006; You et al., 2008) in the atmosphere of
5 urban and semi-urban areas. They are important precursors of secondary organic aerosol (SOA),
6 peroxyacetyl nitrate (PAN), and ozone (Kansal, 2009; Tan et al., 2012; Porter et al., 2017). In
7 addition, many aromatic compounds can cause detrimental effects on human health and plants
8 (Manuela et al., 2012; Sarigiannis and Gotti, 2008; Michalowicz and Duda, 2007).

9 Aromatics are released to the atmosphere by biomass burning as well as fossil fuel evaporation
10 and burning (Cabrera-Perez et al., 2016; Na et al., 2004). The dominant oxidation pathway for
11 aromatics is via reaction with hydroxyl radical (OH, the dominant atmospheric oxidant), followed
12 by reaction with nitrate radical (NO₃) (Cabrera-Perez et al., 2016; and references therein). The
13 corresponding aromatic oxidation products could be involved in many atmospheric chemical
14 processes, which can affect OH recycling and the atmospheric oxidation capacity (Bejan et al.,
15 2006; Chen et al., 2011). A realistic model description of aromatic compounds is necessary to
16 improve our understanding of their effects on the chemistry in the atmosphere. However, up to
17 now few regional or global-scale chemical transport models (CTMs) include detailed aromatic
18 chemistry.

19 Despite the potentially important influence of aromatic compounds on global atmospheric
20 chemistry, their effect on tropospheric ozone formation in polluted urban areas remains largely
21 unknown. The main source and sink processes of tropospheric ozone are photochemical
22 production and loss, respectively (Yan et al., 2016). Observation-based approaches alone cannot
23 provide a full picture of ozone-source attribution for the different NMVOCs. Such ozone-source
24 relationships are needed to improve policymaking strategies to address hemispheric ozone
25 pollution (Chandra et al., 2006). Numerical chemistry-transport models allow us to explore the
26 importance of impacts from aromatics and to attribute observed changes in ozone concentrations
27 to particular sources (Stevenson et al., 2006; Stevenson et al., 2013; Zhang et al., 2014). Current
28 global CTMs reproduce much of the observed regional and seasonal variability in tropospheric
29 ozone concentrations. However, some systematic biases can occur, most commonly an
30 overestimation (Fiore et al., 2009; Reidmiller et al., 2009; Yan et al., 2016, 2018a, b; Ni et al.,
31 2018) due to incomplete representation of physical and chemical processes, and biases in
32 emissions and transport, including the parameterization of small-scale processes and their
33 feedbacks to global-scale chemistry (Yan et al., 2014; Yan et al., 2016).

34 Another motivation for the modeling comes from recent updates in halogen (bromine-chlorine)
35 chemistry, which when implemented in GEOS-Chem decrease the global burden of ozone
36 significantly (by 14%; 2–10 ppb in the troposphere) (Schmidt et al., 2017). This ozone burden
37 decline is driven by decreased chemical ozone production due to halogen-driven nitrogen oxides
38 (NO_x = NO + NO₂) loss; and the ozone decline lowers global mean tropospheric OH
39 concentrations by 11%. Thus GEOS-Chem starts to exhibit low ozone biases compared to



1 ozonesonde observations (Schmidt et al., 2017), particularly in the southern hemisphere,
2 implying that some mechanisms (e.g., due to aromatics) are currently missing from the model.

3 A simplified aromatic oxidation mechanism has previously been employed in GEOS-Chem (e.g.,
4 Fischer et al., 2014; Hu et al., 2015), which is still used in the latest version v11-02. In that
5 simplified treatment, oxidation of benzene (B), toluene (T), and xylene (X) by OH (Atkinson et
6 al., 2000) is assumed to produce first-generation oxidation products ($x\text{RO}_2$, $x = \text{B}, \text{T}, \text{or X}$). And
7 these products further react with hydrogen peroxide (HO_2) or nitric oxide (NO) to produce
8 LxRO_2y ($y = \text{H or N}$), passive tracers which are excluded from tropospheric chemistry. Thus in
9 the presence of NO_x , the overall reaction is aromatic + OH = - NO + (inert tracer). While such a
10 simplified treatment can suffice for budget analyses of the aromatic species themselves, it does
11 not capture ozone production from aromatic oxidation products.

12 In this work, we update the aromatics chemistry in GEOS-Chem based on the SAPRC-11
13 mechanism, and use the updated model to analyze the global and regional scale chemical effects
14 of the most abundant aromatics in the gas phase (benzene, toluene, xylenes) in the troposphere.
15 Specifically, we focus on the impact on ozone formation (due to aromatics oxidation), as this is
16 of great interest for urban areas and can be helpful for developing air pollution control strategies.
17 Further targets are the changes to the NO_x spatial distribution and OH recycling. Model results
18 for aromatics and ozone mixing ratios are evaluated by comparison with observations from
19 surface and aircraft campaigns in order to constrain model accuracy. Finally, we discuss the
20 global effects of aromatics on tropospheric chemistry including ozone, NO_x and HO_x ($\text{HO}_x = \text{OH}$
21 + HO_2).

22 The rest of the paper is organized as follows. Section 2 describes the GEOS-Chem model setups,
23 including the updates in aromatics chemical mechanism. A description of the observational
24 datasets for aromatics and ozone is given in Sect. 3. Section 4 presents the model evaluation for
25 aromatics based on the previously mentioned set of aircraft and surface observations, and
26 evaluates modeled surface ozone with measurements from three networks. An analysis of the
27 tropospheric impacts on ozone, NO_x , and OH, examining the difference between models results
28 with simplified (as in the standard model setup) and with SAPRC-11 aromatic chemistry, is
29 presented in Section 5. Section 6 concludes the present study.

30 2. Model description and setup

31 We use the GEOS-Chem CTM (version 9-02, available at <http://geos-chem.org/>) to interpret the
32 importance of aromatics in tropospheric chemistry and ozone production. A detailed description
33 of the GEOS-Chem model is available at
34 http://acmg.seas.harvard.edu/geos/geos_chem_narrative.html. GEOS-Chem has been used
35 extensively for tropospheric chemistry and transport studies (Zhang and Wang, 2016; Yan et al.,
36 2014; Shen et al., 2015; Lin et al., 2016). Here, the model is run at a horizontal resolution of 2.5°
37 long. x 2° lat. with a vertical grid containing 47 layers (including 10 layers of ~ 130 m thickness



1 each below 850 hPa), as driven by the GEOS-5 assimilated meteorological fields. A non-local
2 scheme implemented by Lin and McElroy (2010) is used for vertical mixing in the planetary
3 boundary layer. Model convection adopts the Relaxed Arakawa-Schubert scheme (Rienecker et
4 al., 2008). Stratospheric ozone production employs the Linoz scheme (McLinden et al., 2000).
5 Dry deposition for aromatic compounds is implemented following the scheme by Hu et al.
6 (2015), which uses a standard resistance-in-series model (Wesely, 1989) and Henry's law
7 constants for benzene (0.18 M atm⁻¹), toluene (0.16 M atm⁻¹), and xylenes (0.15 M atm⁻¹)
8 (Sander, 1999).

9 **2.1 Emissions**

10 Global carbon monoxide (CO) and NO_x anthropogenic emissions are taken from the EDGAR
11 (Emission Database for Global Atmospheric Research) v4.2 inventory. The global inventory has
12 been replaced by regional inventories in China (MEIC, base year: 2008), Asia (excluding China;
13 INTEX-B, 2006), the US (NEI05, 2005), Mexico (BRAVO, 1999), Canada (CAC, 2005), and
14 Europe (EMEP, 2005). Details on these inventories and on the model CO and NO_x anthropogenic
15 emissions are shown in Yan et al. (2016). For anthropogenic NMVOCs including aromatic
16 compounds (benzene, toluene, and xylenes), here we use emission inventory from the RETRO
17 (REanalysis of the TROpospheric chemical composition) (Schultz et al., 2007).

18 The global anthropogenic RETRO (version 2; available at <ftp://ftp.retro.enes.org/>) inventory
19 includes monthly emissions for 24 distinct chemical species during 1960–2000 with a resolution
20 of 0.5° long. × 0.5° lat. (Schultz et al., 2007). It is implemented in GEOS-Chem by regridding to
21 the model resolution (2.5° long. × 2.0° lat.). Emission factors in RETRO are calculated on
22 account of economic and technological considerations. In order to estimate the time dependence
23 of anthropogenic emissions, RETRO also incorporate behavioral aspects (Schultz et al., 2007).
24 The implementation of the monthly RETRO emission inventory in GEOS-Chem is described by
25 Hu et al. (2015), which linked the RETRO species into the corresponding model tracers. The
26 most recent RETRO data (for 2000) is used for the GEOS-Chem model simulation and the
27 calculated annual global anthropogenic NMVOCs are ~ 71 TgC. On a carbon basis, the global
28 aromatics source accounts for ~ 23% (16 TgC) of the total anthropogenic NMVOCs (71 TgC).
29 Figure 1 shows the spatial distribution of anthropogenic emissions for benzene, toluene, and
30 xylenes, respectively. Anthropogenic benzene emissions in Asia (mainly over eastern China and
31 India) are larger than those from other source regions (e.g., over the Europe and eastern US).

32 Biomass burning emissions of aromatics and other chemical species in GEOS-Chem are
33 calculated based on the monthly Global Fire Emission Database version 3 (GFED3) inventory
34 (van der Werf et al., 2010). Natural emissions of NO_x (by lightning and soil) and of biogenic
35 NMVOCs are calculated online by parameterizations driven by model meteorology. Lightning
36 NO_x emissions are parameterized based on cloud top heights (Price and Rind, 1992), and are
37 further constrained by the lightning flash counts detected from satellite instruments (Murray et
38 al., 2012). Soil NO_x emissions are described in Hudman et al. (2012). Biogenic emissions of



1 NMVOCs are calculated by MEGAN (Model of Emissions of Gases and Aerosols from Nature)
2 v2.1 with the Hybrid algorithm (Guenther et al., 2012).

3 **2.2 Updated aromatic chemistry**

4 In the GEOS-Chem model setup, the current standard chemical mechanism with simplified
5 aromatic oxidation chemistry is based on Mao et al. (2013), which is still true for the latest
6 version v11-02. As mentioned in the introduction, this simplified mechanism acts as strong sinks
7 of both HO_x and NO_x, because no HO_x are regenerated in this reaction, and NO is consumed
8 without regenerating NO₂. However, it is reasonably well established that aromatics tend to be
9 radical sources, forming highly reactive products that photolyze to form new radicals, and
10 regenerating radicals in their initial reactions (Carter, 2010a, b; Carter and Heo, 2013). A revised
11 mechanism that takes the general features of aromatics mechanisms into account would be much
12 more reactive, given the reactivity of the aromatic products.

13 This work uses a more detailed and comprehensive aromatics oxidation mechanism: the SAPRC-
14 11 aromatics chemical mechanism. SAPRC-11 is an updated version of the SAPRC-07
15 mechanism (Carter and Heo, 2013), which is consistent with recent literature. Moreover,
16 SAPRC-11 is able to reproduce the ozone formation from aromatic oxidation that is observed in
17 environmental chamber experiments (Carter and Heo, 2013). Table S1 lists new model species in
18 addition to those in the standard GEOS-Chem model setup. Table S2 lists the new reactions and
19 rate constants. In this mechanism, the tropospheric consumption process of aromatics is mainly
20 reaction with OH.

21 As discussed by Carter (2010a, b), aromatic oxidation has two possible OH reaction pathways:
22 OH radical addition and H-atom abstraction (Atkinson, 2000). In SAPRC-11, the reactions
23 following abstraction lead to three different formation products, depending on the participating
24 radical and location of the H-abstraction: an aromatic aldehyde (represented as the *BALD* species
25 in the model), a ketone (*PROD2*), and an aldehyde (*RCHO*). The largest yield of aromatic
26 oxidation corresponds to the reaction after OH addition of aromatic rings. The OH-aromatic
27 adduct is reaction with O₂ either forming HO₂ and a phenolic compound (further consumed by
28 reactions with OH and NO₃ radicals), or to form an OH-aromatic-O₂ adduct. The OH-aromatic-
29 O₂ adduct further undergoes two competing unimolecular reactions to ultimately form OH, HO₂,
30 an α -dicarbonyl (such as glyoxal (*GLY*), methylglyoxal (*MGLY*) or biacetyl (*BACL*)), a
31 monounsaturated dicarbonyl co-product (*AFG1*, *AFG2*, the photoreactive products) and a di-
32 unsaturated dicarbonyl product (*AFG3*, the reactions of uncharacterized non-photoreactive ring
33 fragmentation products) (Calvert et al., 2002).

34 Formed from the phenolic products, the SAPRC-11 mechanism includes species of cresols
35 (*CRES*), phenol (*PHEN*), xlenols, alkyl phenols (*XYNL*), and catechols (*CATL*). Due to their
36 different SOA and ozone formation potentials (Carter et al, 2012), these phenolic species are
37 represented separately. Relatively high yields of catechol (*CATL*) have been observed in the



1 reactions of OH radicals with phenolic compounds. Furthermore, their subsequent reactions are
2 believed to be important for SOA and ozone formation (Carter et al, 2012).

3 **2.3 Simulation setups**

4 In order to investigate the global chemical effects of the most commonly emitted aromatics in the
5 troposphere, two simulations were performed, one with the ozone related aromatic chemistry
6 updates from SAPRC-11 (the SAPRC case), and the other with simplified aromatic chemistry as
7 in the standard setup (the Base case). Both simulations are conducted from July 2004 to
8 December 2005 based on the available observations (Sect. 3). Initial conditions of chemicals are
9 regridded from a simulation at 5° long. × 4° lat. started from 2004. Simulations over July–
10 December 2004 allow for a 6-month spin-up for our focused analysis over the year of 2005. For
11 comparison with aromatics observations over the US in 2010–2011 (Sect. 3), we extend the
12 SAPRC simulation from July 2009 to December 2011.

13 **3. Aromatics and ozone observations**

14 We use a set of measurements from surface and aircraft campaigns to evaluate the model
15 simulated aromatics and ozone.

16 **3.1 Aromatic aircraft observations**

17 For aromatics, we use airborne observations from CALNEX (California; May/June 2010) aircraft
18 study over the US. A proton transfer reaction quadrupole mass spectrometer (PTR-MS) was used
19 to measure mixing ratios of aromatics (and an array of other primary and secondary pollutants)
20 during CALNEX. Measurements are gathered mostly on a one-second time scale (approximately
21 100 m spatial resolution), which permits sampling of the source regions and tracking subsequent
22 transport and transformation throughout California and surrounding regions. Further details of the
23 CALNEX campaign, including the flight track, timeframe, location and instrument, are shown in
24 Hu et al. (2015) and <https://www.esrl.noaa.gov/csd/projects/calnex>.

25 We also employ vertical profiles obtained in 2005 from the CARIBIC (Civil Aircraft for Regular
26 Investigation of the atmosphere Based on an Instrument Container) project, which conducts
27 atmospheric measurements onboard a commercial aircraft (Lufthansa A340-600)
28 (Brenninkmeijer et al., 2007; Baker et al., 2010). CARIBIC flights fly away from Frankfurt,
29 Germany on the way to North America, South America, India and East Asia. Measurements are
30 available in the upper troposphere (50% on average) and lower stratosphere (50%) (UTLS) at
31 altitudes between 10–12 km. To evaluate our results, model data are sampled along the flight
32 tracks, and the annual means from GEOS-Chem model simulations at the 250 hPa level are used
33 to compare with observations between 200–300 hPa.

34 **3.2 Aromatics surface measurements**



1 To evaluate the ground-level mixing ratios of benzene, toluene, and xylenes as well as their
2 seasonal cycles, surface observations of aromatics are collected from two networks (EMEP, data
3 available at <http://www.nilu.no/projects/ccc/emepdata.html>, and the European Environmental
4 Agency (EEA), data available at [http://www.eea.europa.eu/data-and-maps/data/airbase-the-](http://www.eea.europa.eu/data-and-maps/data/airbase-the-european-air-quality-database-8)
5 [european-air-quality-database-8](http://www.eea.europa.eu/data-and-maps/data/airbase-the-european-air-quality-database-8), both for the year 2005) over Europe and the KCMP tall tower
6 dataset (data available at <https://atmoschem.umn.edu/data>, for the year 2011) over the US.

7 EMEP, which aims to investigate the long-range transport of air pollution and the flux through
8 boundaries (Torseth et al., 2012), locates measurement sites at which there are minimal local
9 impacts, thus consequently the observations could represent the feature of large regions. EMEP
10 has a daily resolution with a total of 14 stations located in Europe for benzene, 12 stations for
11 toluene, and 8 stations for xylenes (Table 1). Here we use the monthly values calculated from the
12 database to evaluate monthly model results. Note that measurement speciation of xylenes (o-
13 xylene, m-xylene and p-xylene) in EMEP network does not exactly correspond with the model
14 speciation of xylenes (m-xylene, p-xylene, o-xylene and ethylbenzene) (Hu et al., 2015). The
15 speciation assumption probably can partly account for the xylene model-measurement
16 discrepancy seen in Sect. 4.

17 EEA provides observations from a large number of sites over urban, suburban and background
18 regions (EEA, 2014). However, here we use only rural background sites to do model comparison,
19 as in Cabrera-Perez et al. (2016), because the model horizontal scale cannot simulate direct traffic
20 or industrial influence. This leads to 22 stations available for benzene and 6 stations for toluene.
21 For comparison, annual means for individual site have been used.

22 The KCMP tall tower measurements (at 44.69°N, 93.07°W) have been widely used for studies of
23 surface fluxes of tropospheric trace species and land-atmosphere interactions (Kim et al., 2013;
24 Hu et al., 2015; Chen et al., 2018). A suite of NMVOCs including aromatics were observed at the
25 KCMP tower during 2009–2012 with a high-sensitivity PTR-MS, sampling from a height of 185
26 m above ground level. We use the hourly observations of benzene, toluene and C₈ (xylenes +
27 ethylbenzene; here consistent with the model speciation) aromatics for our model evaluation.

28 3.3 Ozone observations

29 Ozone observations are taken from the database of the World Data Centre for Greenhouse Gases
30 (WDCGG, data available at <http://ds.data.jma.go.jp/gmd/wdcgg/cgi-bin/wdcgg/catalogue.cgi>),
31 the United States Environmental Protection Agency Air Quality System (US EPA AQS, data
32 available at http://aqsdrl.epa.gov/aqsweb/aqstmp/airdata/download_files.html), and the Chemical
33 Coordination Centre of EMEP (EMEP CCC). These networks contain hourly ozone
34 measurements over a total of 1408 urban, suburban or rural sites. We use monthly averaged
35 observations of surface ozone in 2005 to examine the simulated surface ozone from the GEOS-
36 Chem model. Simulated ozone from the lowest layer (centered at ~ 65 m) is sampled from the
37 grid cells corresponding to the ground sites.



1 4. Evaluation of simulated aromatics and ozone

2 In this part, the SAPRC model simulation results of aromatics (benzene, toluene, xylenes and C₈
3 aromatics) and ozone from GEOS-Chem are evaluated with observations. Table 1 summarizes
4 the statistical comparison between measured and simulated concentrations over the monitoring
5 stations described in Sect. 3. To do the statistical calculations, GEOS-Chem simulation results
6 have been sampled along the geographical locations of the measurements. Table 1 includes the
7 number of locations and time resolutions. The number of sites in EEA for xylenes is only 2, thus
8 we do not include their comparison results in Table 1 due to the lack of representativeness.

9 4.1 Surface-level aromatics

10 For the aromatics near the surface mixing ratios over Europe, observed mean benzene (194.0 ppt
11 for EEA and 166.4 ppt for EMEP) and toluene (240.3 ppt for EEA and 133.1 ppt for EMEP)
12 mixing ratios are higher than observed mean xylene concentrations (42.3 ppt for EMEP). In
13 general, the model underestimates EEA and EMEP observations of benzene (by 34% on average)
14 and toluene (by 20% on average). For benzene, the model results systematically underestimate
15 the annual means (36%) compared to the EMEP database, consistent with the model
16 underestimate of the EEA dataset (32%). The model underestimate for toluene compared to the
17 EMEP dataset (15%) is smaller than that relative to the EEA measurements (25%). The
18 simulation overestimates the xylene measurements in EMEP by a factor of 1.9, in part because
19 the model results include ethylbenzene but the observations do not (see Sect. 3.2). The fact that
20 the anthropogenic RETRO emissions (for year 2000) do not correspond to the year of
21 measurement (2005) may contribute to the above model-measurement discrepancies.

22 The modeled spatial variability of aromatics (with standard deviations of 32.1–66.8 ppt) is 18–
23 73% lower than that of the EMEP and EEA observations (41.9–118.4 ppt), probably due to the
24 coarse model resolution. The spatial variability in benzene (46–73% lower) is the most strongly
25 underestimated among the three aromatic species. Unlike benzene, simulated concentrations of
26 toluene show a larger standard deviation (66.8 ppt) than the EEA measurements (59.4 ppt),
27 indicating larger simulated spatial variability. Simulation results are thus poorly spatially
28 correlated with observations ($R = 0.41$ – 0.49). However, the temporal variability of aromatics is
29 well captured by GEOS-Chem with the correlations above 0.7 for most stations.

30 Figure 2 shows a comparison of model results with observations at six stations for benzene,
31 toluene, and xylenes, respectively, following Cabrera-Perez et al. (2016). Model results
32 reproduce the annual cycle at the majority of sites. Aromatics are better simulated in summer
33 than in winter. This feature has been previously found for the climate-chemistry model EMAC
34 for aromatics (Cabrera-Perez et al., 2016) and simpler NMVOCs (Pozzer et al., 2007). In
35 addition, the measurements show larger standard deviations than the GEOS-Chem simulations,
36 with the ratios between the observed and the simulated standard deviations being 2–11.



1 Over the US, annual mean observed concentrations at the KCMP tall tower are 91.5 ppt for
2 benzene, 56.7 ppt for toluene, and 90.3 ppt for C₈ aromatics (Table 1). The model biases for
3 benzene (8.4 ppt; 9.2%) and C₈ aromatics (-1.4 ppt; -1.6%) are much lower than that for toluene
4 (64.5 ppt; 114%). Figure 3 further shows the observed and simulated monthly averaged
5 concentrations of benzene, toluene and C₈ aromatics. The SAPRC simulation reproduces their
6 seasonal cycles, with higher concentrations in winter and lower mixing ratios in summer,
7 consistent with Hu et al. (2015). The model-observation correlations are 0.89, 0.78 and 0.65 for
8 monthly benzene, toluene, and C₈ aromatics, respectively. The large overestimation of modeled
9 toluene is mainly due to simulated high mixing ratios during the cold season (Fig. 3, October to
10 March).

11 4.2 Tropospheric aromatics

12 Table 1 shows that in the UTLS, both CARIBIC observed (16 ppt) and GEOS-Chem modeled
13 (12.3 ppt) benzene mixing ratios are higher than toluene concentrations (3.6 ppt for CARIBIC
14 and 1.5 ppt for GEOS-Chem). For benzene, the model underestimates appear to be smaller in the
15 free troposphere (with an underestimate by 23%) than at the surface (36% for EMEP and 32% for
16 EEA). In contrast to benzene, annual mean concentrations of toluene are underestimated by 58%
17 in the UTLS. The geographical variability of benzene is larger than that for toluene (with
18 standard deviation of 4.2 versus 0.7 ppt in model and 15.8 versus 7.5 ppt in observation),
19 probably because of the shorter lifetime of toluene in combination with the lower concentrations
20 in the UTLS for toluene. The model results show smaller spatial variability than the observations.
21 This underestimation for spatial variability in the free troposphere (over 70%) is higher than that
22 at the surface (not shown).

23 The black lines in Fig. 4 show the tropospheric aromatics profiles during the CALNEX
24 campaign. The measured values peak at an altitude of 0.6–0.8 km, with concentrations decreasing
25 at higher altitudes. Although the concentrations in the lower troposphere for benzene (40–100 ppt
26 below 2 km) are lower than mixing ratios for toluene (70–160 ppt below 2 km) and C₈ aromatics
27 (50–120 ppt below 2 km), the benzene mixing ratios (> 30 ppt) in the free troposphere are much
28 higher than those of toluene and C₈ aromatics (< 10 ppt), mainly due to the longer lifetime of
29 benzene. The SAPRC simulation (red lines in Fig. 4) captures the general vertical variations of
30 CALNEX benzene and toluene, with statistically significant model-observation correlations of
31 0.74 and 0.65 for benzene and toluene, respectively. The model generally overestimates the
32 measured C₈ aromatics below 0.5 km, albeit with an underestimate above 0.5 km, with lower
33 model-observation correlation of 0.37. This overestimation below 0.5 km is also seen for benzene
34 and toluene.

35 4.3 Surface ozone

36 Table 1 shows an average ozone mixing ratio of 34.1 ppb in 2005 over the regional background
37 WDCGG sites. The annual mean ozone mixing ratios are lower over Europe (from the EMEP



1 dataset), about 30.6 ppb. The ozone mixing ratios are relatively lowest over the US, with an
2 average value of 24.2 ppb, partly due to inclusion of urban and suburban sites that undergo strong
3 titration especially in the cold season. The average over the US rural sites is 32.5 ppb. The
4 SAPRC simulation tends to overestimate the ozone mixing ratios over the US (with a mean bias
5 of +12.1 ppb), whereas it underestimates the mixing ratios over the sites of Europe and
6 background regions with biases of -2.9 ppb and -5.5 ppb, respectively. Figure 5 shows the
7 spatial distribution of the annual mean model biases with respect to the measurements. Unlike the
8 modeled surface aromatics, the simulated ozone spatial variability can be either slightly lower or
9 higher than the observed variability, depending on the compared database: the standard deviation
10 is 10.2 ppb (simulated) versus 13.1 ppb (observed) for AQS sites, 12.8 versus 14.2 ppb for
11 WDCGG sites, 13.2 versus 10.3 ppb for EMEP sites. The temporal variability (temporal
12 correlations of 0.68–0.92) is better captured by the model than the spatial variability (spatial
13 correlations of 0.43–0.54).

14 5. Global effects of aromatic chemistry

15 This section compares the Base and SAPRC simulations to assess to which extent the updated
16 mechanism for aromatics affect the global simulation of ozone, HO_x and individual nitrogen
17 species. Our focus here is on the large-scale impacts.

18 5.1 NO_y Species

19 Figure 6 and Table 2 show the changes from Base to SAPRC in annual average surface NO
20 mixing ratios. A decrease in NO is apparent over NO_x source regions, e.g., by approximately 0.15
21 ppb (~20%) over much of the US, Europe and China (Fig. 6). In contrast, surface NO increases at
22 locations downwind from NO_x source regions (up to ~0.1 ppb or 20%), including the oceanic
23 area off the eastern US coast, the marine area adjacent to Japan, and the Mediterranean area. The
24 change is negligible (by -0.2%) for the annual global mean surface NO (Table 2). Seasonally, the
25 decrease in spring, summer and fall is compensated partly by the increase in winter (Table 2).

26 The zonal average results in Fig. 7 show a clear decline in NO in the planetary boundary layer, in
27 contrast to significant increases in the free troposphere, from Base to SAPRC. The free
28 tropospheric NO increases are largest in the remote northern regions with an annual average
29 enhancement up to 5% (Fig. 7), and are particularly large in winter (up to 10%, not shown). For
30 the whole troposphere, the average NO increases by 0.6% from Base to SAPRC (Table 2).

31 Figure 6 shows that simulated surface NO₂ mixing ratios in the SAPRC scenario are enhanced
32 over most locations throughout the troposphere, in comparison with the Base simulation. Over
33 the source regions, the changes are mixed, with increases in some highly NO_x polluted regions
34 (by up to 10%) and decreases in other polluted regions. On a global mean basis, NO₂ is increased
35 (by 2.1% in the free troposphere and 1.0% at the surface, Table 2), due mainly to the recycling of
36 NO_x from PAN associated with the aromatics, and the reactions of oxidation products from



1 aromatics with NO or NO₃ (primarily) to form NO₂ and HO₂. Combing the changes in NO and
2 NO₂ means that the total NO_x mixing ratios decrease in source regions but increase in the remote
3 free troposphere.

4 The NO₃ mixing ratios decrease at the global scale (−4.1% on average in the troposphere, Fig. 7
5 and Table 2) in the SAPRC simulation, except for an enhancement in surface NO₃ over the
6 northern polar regions and most polluted areas like the eastern US, Europe and eastern China
7 (Fig. 6).

8 Table 2 shows that nitric acid (HNO₃) increases in the SAPRC simulation, both near the surface
9 (by approximately 1.1%) and in the troposphere (by 0.3%). The enhancement in HNO₃ appears
10 uniformly over most continental regions in the northern hemisphere (not shown), due to the
11 promotion of direct formation of HNO₃ from aromatics in the SAPRC simulation.

12 **5.2 OH and HO₂**

13 Compared to the Base simulation, OH increases slightly by 1.1% at the surface in the SAPRC
14 simulation (Fig. 8 and Table 2). The largest increases in OH concentrations are found over source
15 regions dominated by anthropogenic emissions (i.e., the US, Europe, and Asia) and in subtropical
16 continental regions with large biogenic aromatic emissions. In these locations, the peroxy radicals
17 formed by aromatic oxidation react with NO₂ and HO₂, which can have a significant effect on the
18 ambient ozone and NO_x mixing ratios. This in turn influences OH, as the largest photochemical
19 sources of OH are the photolysis of O₃ as well as the reaction of NO with HO₂. Seasonally, a few
20 surface locations see OH concentration increases of more than 10% during April–August (not
21 shown), including parts of the eastern US, central Europe, eastern Asia and Japan.

22 The OH enhancement (0.2%) is also seen in the free troposphere in the SAPRC simulation (Fig. 9
23 and Table 2). OH is increased in the troposphere of the northern hemisphere, in contrast to the
24 decline in the troposphere of tropics and southern hemisphere (Fig. 9). These OH changes
25 correspond to the hemispherically distinct changes in aromatics (benzene, toluene, and xylenes),
26 which show a decrease in the northern hemisphere, an increase in the southern hemisphere, and
27 an increase in global mean (by 1%) (not shown). Despite the overall increase in tropospheric OH,
28 CO is increased by ~1% (Table 2) due to additional formation from aromatics oxidation.

29 Table 2 shows that from Base to SAPRC, HO₂ shows a significant increase at the global scale:
30 3.0% at the surface and 1.3% in the troposphere, due to regeneration of HO_x from aromatics
31 oxidation products. Correspondingly, the OH/HO₂ ratio decreases slightly. These changes mean
32 that, compared to the simplified aromatic chemistry in the standard model setup, the SAPRC
33 mechanism are associated with higher OH (i.e., more chemically reactive troposphere) and even
34 higher HO₂.

35 **5.3 Ozone**



1 From Base to SAPRC, the global average surface ozone mixing ratio increases by less than 1%
2 (Table 2). This small difference is comparable to the result calculated by Cabrera-Perez et al.
3 (2017) with the EMAC model, which is based on a reduced version of the aromatic chemistry
4 from the Master Chemical Mechanism (MCMv3.2). Figure 8 shows that the 1% increase in
5 surface ozone occurs generally over the northern hemisphere. Similar to the changes in OH, the
6 most notable ozone increase occurs in industrially-polluted regions. These regions show
7 significant local ozone photochemical formation in both the Base case and the SAPRC
8 simulation. The updated aromatic chemistry increases ozone by up to 5 ppb in these regions.
9 Increases of ozone are much smaller (less than 0.2 ppb) over the tropical oceans than in the
10 continental areas. In contrast, ozone declines in regions dominated by emissions from biomass
11 burning over the southern hemisphere. Changes elsewhere in the troposphere are similar in
12 magnitude, as shown in Figure 9.

13 Two general factors likely contribute to the ozone change from Base to SAPRC. In the SAPRC
14 simulation, the addition of aromatic oxidation products (i.e., peroxy radicals) can contribute
15 directly to ozone formation in NO_x-rich source regions and also in the NO_x-sensitive remote
16 troposphere (i.e., from PAN to NO_x and to ozone). The second factor is a change in the NO_x
17 spatial distribution, with an overall enhancement in average NO₂ concentrations. The
18 redistribution is mainly caused by enhanced transport of NO_x to the remote troposphere (see Sect.
19 5.1). The enhanced NO_x in the remote troposphere enhances the overall ozone formation because
20 this process is more efficient in the remote regions (e.g., Liu et al., 1987). The increased ozone,
21 NO₂ and NO_x transport all lead to the aforementioned changes. This is described in detail in
22 section 5.4.

23 There are notable decreases (more than 5%, Fig. 9) in simulated ozone and OH in the free
24 troposphere (above 4 km) over the tropics (30°S–30°N). A similar decrease is found in modeled
25 NO_x (above 6 km, Fig. 7). These decreases are probably related to the upward transport of
26 aromatics (mainly benzene, whose lifetime is longer than the other two species) by tropical
27 convection processes. The aromatics transported to the upper troposphere may cause net
28 consumption of tropospheric OH and NO_x, which can further reduce ozone production.

29 From Base to SAPRC, the modeled ozone concentrations are closer to the WDCGG and EMEP
30 network measurements, but the agreement worsens at the AQS sites (Table 3). For the WDCGG
31 background sites, the annual and seasonal model biases are ~10% smaller in the SAPRC
32 simulation compared to the Base case. For the EMEP stations, although the model results are not
33 improved in summer and fall, the annual model bias is 25% smaller (–2.8 ppb versus –3.5 ppb) in
34 the SAPRC simulation. There are significant overestimates in the Base simulation at the AQS
35 sites, with an annual mean bias of 11.4 ppb. This model overestimation is consistent with the
36 results of previous works (Yan et al., 2016; Fiore et al., 2009; Reidmiller et al., 2009). The recent
37 study of Schmidt et al. (2017) includes a more comprehensive representation of multiphase
38 halogen (Br–Cl) chemistry in GEOS-Chem, which causes a 14% decrease in the global burden of
39 tropospheric ozone and negative ozone biases over the US. Past studies have suggested that the



1 model biases (positive in most models) are a multifaceted problem, such as the effect of coarse
2 resolution and how small-scale processes are represented (Yan et al., 2016).

3 **5.4 Discussion of SAPRC aromatic-ozone chemistry**

4 As discussed in Sect. 5.3, the increased O₃ mixing ratios from Base to SAPRC are due to the
5 direct impact of aromatic oxidation products (i.e., peroxy radicals) and to the effect of increased
6 NO₂ concentrations. The simulated odd oxygen family (O_x = O₃ + O(¹D) + O(³P) + NO₂ +
7 2×NO₃ + 3×N₂O₅ + HNO₃ + HNO₄ + PAN, Wu et al., 2007; Yan et al., 2016) formation
8 increases by 1–10%, both over the source regions and in the remote troposphere. Although the
9 percentage changes are similar, the driving factors over the source regions are different from the
10 drivers in the remote troposphere.

11 Regions with large aromatics emissions show a significant increase of oxidation products from
12 Base to SAPRC. The modeled ozone in these regions increases with increasing NO₂ and its
13 oxidation products. NO and NO₃ are often lower in these regions in the SAPRC scenario because
14 of their reactions with the aromatic-OH oxidation products to form NO₂ and HO₂. In remote
15 regions and in the free troposphere, ozone production is also enhanced by both NO₂ and HO₂
16 increases in the SAPRC simulation, but the increase in ozone formation is mainly attributed to
17 the increase in NO_x mixing ratios.

18 NO_x concentrations decrease in source regions and increase in the remote regions because of
19 more efficient transport of PAN and its analogues (represented by *PBZN* here in SAPRC-11). In
20 the SAPRC-11 aromatics chemical scheme the immediate precursor of PAN (peroxyacetyl
21 radical) has five dominant photochemical precursors. They are acetone (CH₃COCH₃, model
22 species: *ACET*), methacrolein (*MACR*), biacetyl (*BACL*), methyl glyoxal (*MGLY*) and other
23 ketones (e.g., *PROD2*, *AFGI*). These compounds explain the increased rate of PAN formation.
24 For example, the SAPRC simulation has increased the concentration of *MGLY* by a factor of 2. In
25 addition, production of organic nitrates (Table S2) in the model with SAPRC aromatics chemistry
26 may also explain the increase in ambient NO_x in the remote regions, due to the re-release of NO_x
27 from organic nitrates (as opposed to removal by deposition). Due to recycling of NO_x from PAN-
28 like compounds and also transport of NO_x, NO_x increases by up to 5% at the surface in most
29 remote regions and by ~1% in the troposphere as a whole. This then leads to increased ozone due
30 to the effectiveness of ozone formation in the free troposphere.

31 **6. Conclusions**

32 A representation of tropospheric reactions for aromatic hydrocarbons in the SAPRC-11
33 mechanism has been added to GEOS-Chem, to give a more realistic representation of their
34 atmospheric chemistry. The GEOS-Chem simulation with the SAPRC-11 aromatics mechanism
35 has been evaluated against measurements from aircraft and surface campaigns. The comparison
36 with observations shows reasonably good agreement for aromatics (benzene, toluene, and



1 xylenes) and ozone. Model results for aromatics can reproduce the seasonal cycle, with a general
2 underestimate over Europe for benzene and toluene, and an overestimate of xylenes; while over
3 the US a positive model bias for benzene and toluene and a negative bias for C₈ aromatics are
4 found. From the Base to the SAPRC simulation, the model ozone bias is reduced by 10% relative
5 to WDCGG observations and by 25% relative to EMEP observations, although the bias increases
6 by 5% at the AQS sites.

7 The simplified aromatics chemistry in the Base simulation under-predicts NO and NO₃ oxidation,
8 and it does not represent ozone formed from aromatic-OH-NO_x oxidation. Although the global
9 average changes in simulated chemical species are relatively small (1%–4% from Base to
10 SAPRC), on a regional scale the differences can be much larger, especially over aromatics and
11 NO_x source regions. From Base to SAPRC, NO₂ is enhanced by up to 10% over some highly
12 polluted areas, while reductions are notable in other polluted areas. Although the simulated
13 surface NO decreases by approximately 0.15 ppb (~20%) or more in the northern hemispheric
14 source regions, including most of the US, Europe and China, increases are found (~0.1 ppb, up to
15 20%) at locations downwind from these source regions. The total NO_x mixing ratios decrease in
16 source regions but increase in the remote free troposphere. This is mainly due to the addition of
17 aromatics oxidation products in the model that lead to PAN, which facilitates the transport of
18 nitrogen oxides to downwind locations remote from the sources. Finally, the updated aromatic
19 chemistry in GEOS-Chem increases ozone concentrations, especially over industrialized regions
20 (up to 5 ppb, or more than 10%). Ozone changes in the model are partly explained by the direct
21 impact of increased aromatic oxidation products (i.e., peroxy radical), and partly by the effect of
22 the altered spatial distribution of NO_x. Overall, our results suggest that a better representation of
23 aromatics chemistry is important to model the tropospheric oxidation capacity.

24 **Data Availability**

25 The GEOS-Chem code used to generate this paper and the model results are available upon
26 request. The aircraft and surface data used in this paper is already publically available. Airborne
27 observations of aromatics from CALNEX (<https://www.esrl.noaa.gov/csd/projects/calnex>) and
28 CARIBIC project. Surface observations of aromatics are collected from EMEP
29 (<http://www.nilu.no/projects/ccc/emepdata.html>) and EEA ([http://www.eea.europa.eu/data-and-](http://www.eea.europa.eu/data-and-maps/data/airbase-the-european-air-quality-database-8)
30 [maps/data/airbase-the-european-air-quality-database-8](http://www.eea.europa.eu/data-and-maps/data/airbase-the-european-air-quality-database-8)) over Europe and the KCMP tall tower
31 dataset (<https://atmoschem.umn.edu/data>) over the US. Ozone observations are taken from
32 WDCGG (<http://ds.data.jma.go.jp/gmd/wdcgg/cgi-bin/wdcgg/catalogue.cgi>), AQS
33 (http://aqsd1.epa.gov/aqsweb/aqstmp/airdata/download_files.html), and EMEP.

34 **Acknowledgements**

35 This research is supported by the National Natural Science Foundation of China (41775115) and
36 the 973 program (2014CB441303). We acknowledge the free use of ozone data from networks of
37 WDCGG (<http://ds.data.jma.go.jp/gmd/wdcgg/cgi-bin/wdcgg/catalogue.cgi>), EMEP



1 (<http://www.nilu.no/projects/ccc/emepdata.html>), and AQS
2 (http://aqsdrl.epa.gov/aqsweb/aqstmp/airdata/download_files.html) and aromatic compounds
3 observations from EEA ([http://www.eea.europa.eu/data-and-maps/data/airbase-the-european-air-](http://www.eea.europa.eu/data-and-maps/data/airbase-the-european-air-quality-database-8)
4 [quality-database-8](http://www.eea.europa.eu/data-and-maps/data/airbase-the-european-air-quality-database-8)) and EMEP. We also want to thank Angela Baker for providing the CARIBIC
5 data. DBM acknowledges support from NASA (Grant #NNX14AP89G).

6 Reference

- 7 EEA: Air quality in Europe - 2014 report, Report No. 5/2014, European Environment Agency,
8 Copenhagen, DK, available at: [http://www.eea.europa.eu/publications/air-quality-in-europe-](http://www.eea.europa.eu/publications/air-quality-in-europe-2014)
9 2014, 2014.
- 10 Carter, W. P. L., Goo young Heo, David R. Cocker III, and Shunsuke Nakao (2012): “SOA
11 Formation: Chamber Study and Model Development,” Final report to CARB contract 08-326,
12 May 21. Available at <http://www.cert.ucr.edu/~carter/absts.htm>
- 13 Calvert, J. G., R. Atkinson, K. H. Becker, R. M. Kamens, J. H. Seinfeld, T. J. Wallington and G.
14 Yarwood (2002): “The Mechanisms of Atmospheric Oxidation of Aromatic Hydrocarbons,”
15 Oxford University Press, New York, 566p.
- 16 Carter, W. P. L. (2010a): “Development of the SAPRC-07 Chemical Mechanism and Updated
17 Ozone Reactivity Scales,” Final report to the California Air Resources Board Contract No. 03-
18 318, 06-408, and 07-730. January 27. Available at www.cert.ucr.edu/~carter/SAPRC.
- 19 Carter, W. P. L. (2010b): “Development of the SAPRC-07 chemical mechanism,” *Atmospheric*
20 *Environment* 44, 5324-5335.
- 21 Carter, W. P. L., and Heo, G.: Development of revised SAPRC aromatics mechanisms,
22 *Atmospheric Environment*, 77, 404-414, [10.1016/j.atmosenv.2013.05.021](https://doi.org/10.1016/j.atmosenv.2013.05.021), 2013.
- 23 Sander, R. (1999), *Compilation of Henry’s law constants for inorganic and organic species of*
24 *potential importance in environmental chemistry (Version 3)*, available at [http://www.henryslaw-](http://www.henryslaw.org)
25 [law.org](http://www.henryslaw.org).
- 26 Schultz, M., L. Backman, Y. Balkanski, S. Bjoerndalsaeter, R. Brand, J. Burrows, S. Dalsoeren,
27 M. de Vasconcelos, B. Grodtmann, and D. Hauglustaine (2007), *REanalysis of the TROpospheric*
28 *chemical composition over the past 40 years (RETRO)—A long-term global modeling study of*
29 *tropospheric chemistry: Final report, Jülich/Hamburg, Germany.*
- 30 M.M. Rienecker, M.J. Suarez, R. Todling, J. Bacmeister, L. Takacs, H.-C. Liu, W. Gu, M.
31 Sienkiewicz, R.D. Koster, R. Gelaro, I. Stajner, E. Nielsen *The GEOS-5 Data Assimilation*
32 *System - Documentation of Versions 5.0.1, 9.1.0, and 5.2.0*, NASA, 2008
- 33 Seinfeld, J. H. and Pandis, S. N.: *Atmospheric chemistry and physics: from air pollution to*
34 *climate change*, John Wiley & Sons, 2012.



- 1 Atkinson, R.: Atmospheric chemistry of VOCs and NO_x, *Atmospheric Environment*, 34, 2063-
2 2101, 10.1016/s1352-2310(99)00460-4, 2000.
- 3 Baker, A. K., Slemr, F., and Brenninkmeijer, C. A. M.: Analysis of non-methane hydrocarbons in
4 air samples collected aboard the CARIBIC passenger aircraft, *Atmospheric Measurement*
5 *Techniques*, 3, 311-321, 2010.
- 6 Bejan, I., Abd El Aal, Y., Barnes, I., Benter, T., Bohn, B., Wiesen, P., and Kleffmann, J.: The
7 photolysis of ortho-nitrophenols: a new gas phase source of HONO, *Physical Chemistry*
8 *Chemical Physics*, 8, 2028-2035, 10.1039/b516590c, 2006.
- 9 Brenninkmeijer, C. A. M., Crutzen, P., Boumard, F., Dauer, T., Dix, B., Ebinghaus, R., Filippi,
10 D., Fischer, H., Franke, H., Friess, U., Heintzenberg, J., Helleis, F., Hermann, M., Kock, H. H.,
11 Koepfel, C., Lelieveld, J., Leuenberger, M., Martinsson, B. G., Miemczyk, S., Moret, H. P.,
12 Nguyen, H. N., Nyfeler, P., Oram, D., O'Sullivan, D., Penkett, S., Platt, U., Pucek, M., Ramonet,
13 M., Randa, B., Reichelt, M., Rhee, T. S., Rohwer, J., Rosenfeld, K., Scharffe, D., Schlager, H.,
14 Schumann, U., Slemr, F., Sprung, D., Stock, P., Thaler, R., Valentino, F., van Velthoven, P.,
15 Waibel, A., Wandel, A., Waschitschek, K., Wiedensohler, A., Xueref-Remy, I., Zahn, A., Zech,
16 U., and Ziereis, H.: Civil Aircraft for the regular investigation of the atmosphere based on an
17 instrumented container: The new CARIBIC system, *Atmospheric Chemistry and Physics*, 7,
18 4953-4976, 2007.
- 19 Cabrera-Perez, D., Taraborrelli, D., Sander, R., and Pozzer, A.: Global atmospheric budget of
20 simple monocyclic aromatic compounds, *Atmospheric Chemistry and Physics*, 16, 6931-6947,
21 10.5194/acp-16-6931-2016, 2016.
- 22 Chandra, A., Pradhan, P., Tewari, R., Sahu, S., and Shenoy, P.: An observation-based approach
23 towards self-managing web servers, *Computer Communications*, 29, 1174-1188,
24 10.1016/j.comcom.2005.07.003, 2006.
- 25 Chen, J., Wenger, J. C., and Venables, D. S.: Near-Ultraviolet Absorption Cross Sections of
26 Nitrophenols and Their Potential Influence on Tropospheric Oxidation Capacity, *Journal of*
27 *Physical Chemistry A*, 115, 12235-12242, 10.1021/jp206929r, 2011.
- 28 Chen, Z., T.J. Griffis, J.M. Baker, D.B. Millet, J.D. Wood, E.J. Dlugokencky, A.E. Andrews, C.
29 Sweeney, C. Hu, and R.K. Kolka (2018), Source partitioning of methane emissions and its
30 seasonality in the U.S. Midwest, *J. Geophys. Res.*, 123, doi:10.1002/2017JG004356.
- 31 Fiore, A. M., Dentener, F. J., Wild, O., Cuvelier, C., Schultz, M. G., Hess, P., Textor, C., Schulz,
32 M., Doherty, R. M., Horowitz, L. W., MacKenzie, I. A., Sanderson, M. G., Shindell, D. T.,
33 Stevenson, D. S., Szopa, S., Van Dingenen, R., Zeng, G., Atherton, C., Bergmann, D., Bey, I.,
34 Carmichael, G., Collins, W. J., Duncan, B. N., Faluvegi, G., Folberth, G., Gauss, M., Gong, S.,
35 Hauglustaine, D., Holloway, T., Isaksen, I. S. A., Jacob, D. J., Jonson, J. E., Kaminski, J. W.,
36 Keating, T. J., Lupu, A., Marmer, E., Montanaro, V., Park, R. J., Pitari, G., Pringle, K. J., Pyle, J.



- 1 A., Schroeder, S., Vivanco, M. G., Wind, P., Wojcik, G., Wu, S., and Zuber, A.: Multimodel
2 estimates of intercontinental source-receptor relationships for ozone pollution, *Journal of*
3 *Geophysical Research*, 114, 10.1029/2008jd010816, 2009.
- 4 Fischer, E. V., Jacob, D. J., Yantosca, R. M., Sulprizio, M. P., Millet, D. B., Mao, J., Paulot, F.,
5 Singh, H. B., Roiger, A., Ries, L., Talbot, R. W., Dzepina, K., and Pandey Deolal, S.:
6 Atmospheric peroxyacetyl nitrate (PAN): a global budget and source attribution, *Atmos. Chem.*
7 *Phys.*, 14, 2679-2698, <https://doi.org/10.5194/acp-14-2679-2014>, 2014.
- 8 Guenther, A.: Estimates of global terrestrial isoprene emissions using MEGAN (Model of
9 Emissions of Gases and Aerosols from Nature) (vol 6, pg 3181, 2006), *Atmospheric Chemistry*
10 *and Physics*, 7, 4327-4327, 2007.
- 11 Guenther, A. B., Jiang, X., Heald, C. L., Sakulyanontvittaya, T., Duhl, T., Emmons, L. K., and
12 Wang, X.: The Model of Emissions of Gases and Aerosols from Nature version 2.1
13 (MEGAN2.1): an extended and updated framework for modeling biogenic emissions,
14 *Geoscientific Model Development*, 5, 1471-1492, 10.5194/gmd-5-1471-2012, 2012.
- 15 Guo, H., Wang, T., Blake, D. R., Simpson, I. J., Kwok, Y. H., and Li, Y. S.: Regional and local
16 contributions to ambient non-methane volatile organic compounds at a polluted rural/coastal site
17 in Pearl River Delta, China, *Atmospheric Environment*, 40, 2345-2359,
18 10.1016/j.atmosenv.2005.12.011, 2006.
- 19 Hu, L., Millet, D. B., Baasandorj, M., Griffis, T. J., Travis, K. R., Tessum, C. W., Marshall, J. D.,
20 Reinhard, W. F., Mikoviny, T., Muller, M., Wisthaler, A., Graus, M., Warneke, C., and de Gouw,
21 J.: Emissions of C-6-C-8 aromatic compounds in the United States: Constraints from tall tower
22 and aircraft measurements, *Journal of Geophysical Research-Atmospheres*, 120, 826-842,
23 10.1002/2014jd022627, 2015.
- 24 Hudman, R. C., Moore, N. E., Mebust, A. K., Martin, R. V., Russell, A. R., Valin, L. C., and
25 Cohen, R. C.: Steps towards a mechanistic model of global soil nitric oxide emissions:
26 implementation and space based-constraints, *Atmospheric Chemistry and Physics*, 12, 7779-
27 7795, 10.5194/acp-12-7779-2012, 2012.
- 28 Kansal, A.: Sources and reactivity of NMHCs and VOCs in the atmosphere: A review, *Journal of*
29 *Hazardous Materials*, 166, 17-26, 10.1016/j.jhazmat.2008.11.048, 2009.
- 30 Kim, S.Y., D.B. Millet, L. Hu, M.J. Mohr, T.J. Griffis, D. Wen, J.C. Lin, S.M. Miller, and M.
31 Longo (2013), Constraints on carbon monoxide emissions based on tall tower measurements in
32 the US Upper Midwest, *Environ. Sci. Technol.*, 47, 8316-8324.
- 33 Lin, J. T., and McElroy, M. B.: Impacts of boundary layer mixing on pollutant vertical profiles in
34 the lower troposphere: Implications to satellite remote sensing, *Atmospheric Environment*, 44,
35 1726-1739, 10.1016/j.atmosenv.2010.02.009, 2010.



- 1 Lin, J.-T., Tong, D., Davis, S., Ni, R.-J., Tan, X., Pan, D., Zhao, H., Lu, Z., Streets, D., Feng, T.,
2 Zhang, Q., Yan, Y.-Y., Hu, Y., Li, J., Liu, Z., Jiang, X., Geng, G., He, K., Huang, Y., and Guan,
3 D.: Global climate forcing of aerosols embodied in international trade, *Nature Geoscience*, 9,
4 790-794, doi:10.1038/NGEO2798, 2016.
- 5 Manuela, C., Gianfranco, T., Maria, F., Tiziana, C., Carlotta, C., Giorgia, A., Assunta, C., Pia, S.
6 M., Jean-Claude, A., Francesco, T., and Angela, S.: Assessment of occupational exposure to
7 benzene, toluene and xylenes in urban and rural female workers, *Chemosphere*, 87, 813-819,
8 10.1016/j.chemosphere.2012.01.008, 2012.
- 9 McLinden, C. A., Olsen, S. C., Hannegan, B., Wild, O., Prather, M. J., and Sundet, J.:
10 Stratospheric ozone in 3-D models: A simple chemistry and the cross-tropopause flux, *Journal of*
11 *Geophysical Research-Atmospheres*, 105, 14653-14665, 10.1029/2000jd900124, 2000.
- 12 Michalowicz, J., and Duda, W.: Phenols - Sources and toxicity, *Polish Journal of Environmental*
13 *Studies*, 16, 347-362, 2007.
- 14 Murray, L. T., Jacob, D. J., Logan, J. A., Hudman, R. C., and Koshak, W. J.: Optimized regional
15 and interannual variability of lightning in a global chemical transport model constrained by
16 LIS/OTD satellite data, *Journal of Geophysical Research-Atmospheres*, 117,
17 10.1029/2012jd017934, 2012.
- 18 Murray, L. T., Logan, J. A., and Jacob, D. J.: Interannual variability in tropical tropospheric
19 ozone and OH: The role of lightning, *Journal of Geophysical Research-Atmospheres*, 118,
20 11468-11480, 10.1002/jgrd.50857, 2013.
- 21 Na, K., Kim, Y. P., Moon, I., and Moon, K. C.: Chemical composition of major VOC emission
22 sources in the Seoul atmosphere, *Chemosphere*, 55, 585-594,
23 10.1016/j.chemosphere.2004.01.010, 2004.
- 24 Ni, R., Lin, J., Yan, Y., and Lin, W.: Foreign and domestic contributions to springtime ozone
25 over China, *Atmos. Chem. Phys. Discuss.*, <https://doi.org/10.5194/acp-2017-1226>, in review,
26 2018.
- 27 Porter, W. C., Safieddine, S. A., and Heald, C. L.: Impact of aromatics and monoterpenes on
28 simulated tropospheric ozone and total OH reactivity, *Atmospheric Environment*, 169, 250-257,
29 10.1016/j.atmosenv.2017.08.048, 2017
- 30 Price, C., and Rind, D.: A simple lightning parameterization for calculating global lightning
31 distributions, *J. Geophys. Res.-Atmos.*, 97, 9919-9933, <https://doi.org/10.1029/92JD00719>, 1992.
- 32 Ran, L., Zhao, C. S., Geng, F. H., Tie, X. X., Tang, X., Peng, L., Zhou, G. Q., Yu, Q., Xu, J. M.,
33 and Guenther, A.: Ozone photochemical production in urban Shanghai, China: Analysis based on
34 ground level observations, *Journal of Geophysical Research-Atmospheres*, 114,
35 10.1029/2008jd010752, 2009.



- 1 Reidmiller, D. R., Fiore, A. M., Jaffe, D. A., Bergmann, D., Cuvelier, C., Dentener, F. J.,
2 Duncan, B. N., Folberth, G., Gauss, M., Gong, S., Hess, P., Jonson, J. E., Keating, T., Lupu, A.,
3 Marmer, E., Park, R., Schultz, M. G., Shindell, D. T., Szopa, S., Vivanco, M. G., Wild, O., and
4 Zuber, A.: The influence of foreign vs. North American emissions on surface ozone in the US,
5 *Atmospheric Chemistry and Physics*, 9, 5027-5042, 2009.
- 6 Sarigiannis, D. A., and Gotti, A.: BIOLOGY-BASED DOSE-RESPONSE MODELS FOR
7 HEALTH RISK ASSESSMENT OF CHEMICAL MIXTURES, *Fresenius Environmental*
8 *Bulletin*, 17, 1439-1451, 2008.
- 9 Schmidt, J. A. ; Jacob, D. J. ; Horowitz, H. M. ; Hu, L. ; Sherwen, T. ; Evans, M. J. ; Liang, Q. ;
10 Suleiman, R. M. ; Oram, D. E. ; LeBreton, M. ; et al. Modeling the tropospheric BrO background:
11 importance of multiphase chemistry and implications for ozone, OH, and mercury. *J. Geophys.*
12 *Res.* Submitted.
- 13 Shen, L., Mickley, L. J., and Tai, A. P. K.: Influence of synoptic patterns on surface ozone
14 variability over the eastern United States from 1980 to 2012, *Atmospheric Chemistry and*
15 *Physics*, 15, 10925-10938, [10.5194/acp-15-10925-2015](https://doi.org/10.5194/acp-15-10925-2015), 2015.
- 16 Stevenson, D. S., Dentener, F. J., Schultz, M. G., Ellingsen, K., van Noije, T. P. C., Wild, O.,
17 Zeng, G., Amann, M., Atherton, C. S., Bell, N., Bergmann, D. J., Bey, I., Butler, T., Cofala, J.,
18 Collins, W. J., Derwent, R. G., Doherty, R. M., Drevet, J., Eskes, H. J., Fiore, A. M., Gauss, M.,
19 Hauglustaine, D. A., Horowitz, L. W., Isaksen, I. S. A., Krol, M. C., Lamarque, J. F., Lawrence,
20 M. G., Montanaro, V., Müller, J. F., Pitari, G., Prather, M. J., Pyle, J. A., Rast, S., Rodriguez, J.
21 M., Sanderson, M. G., Savage, N. H., Shindell, D. T., Strahan, S. E., Sudo, K., and Szopa, S.:
22 Multimodel ensemble simulations of present-day and near-future tropospheric ozone, *Journal of*
23 *Geophysical Research*, 111, [10.1029/2005jd006338](https://doi.org/10.1029/2005jd006338), 2006.
- 24 Stevenson, D. S., Young, P. J., Naik, V., Lamarque, J. F., Shindell, D. T., Voulgarakis, A., Skeie,
25 R. B., Dalsoren, S. B., Myhre, G., Berntsen, T. K., Folberth, G. A., Rumbold, S. T., Collins, W.
26 J., MacKenzie, I. A., Doherty, R. M., Zeng, G., van Noije, T. P. C., Strunk, A., Bergmann, D.,
27 Cameron-Smith, P., Plummer, D. A., Strode, S. A., Horowitz, L., Lee, Y. H., Szopa, S., Sudo, K.,
28 Nagashima, T., Josse, B., Cionni, I., Righi, M., Eyring, V., Conley, A., Bowman, K. W., Wild,
29 O., and Archibald, A.: Tropospheric ozone changes, radiative forcing and attribution to emissions
30 in the Atmospheric Chemistry and Climate Model Intercomparison Project (ACCMIP),
31 *Atmospheric Chemistry and Physics*, 13, 3063-3085, [10.5194/acp-13-3063-2013](https://doi.org/10.5194/acp-13-3063-2013), 2013.
- 32 Tan, J. H., Guo, S. J., Ma, Y. L., Yang, F. M., He, K. B., Yu, Y. C., Wang, J. W., Shi, Z. B., and
33 Chen, G. C.: Non-methane Hydrocarbons and Their Ozone Formation Potentials in Foshan,
34 China, *Aerosol and Air Quality Research*, 12, 387-398, [10.4209/aaqr.2011.08.0127](https://doi.org/10.4209/aaqr.2011.08.0127), 2012.
- 35 Torseth, K., Aas, W., Breivik, K., Fjaeraa, A. M., Fiebig, M., Hjellbrekke, A. G., Myhre, C. L.,
36 Solberg, S., and Yttri, K. E.: Introduction to the European Monitoring and Evaluation Programme

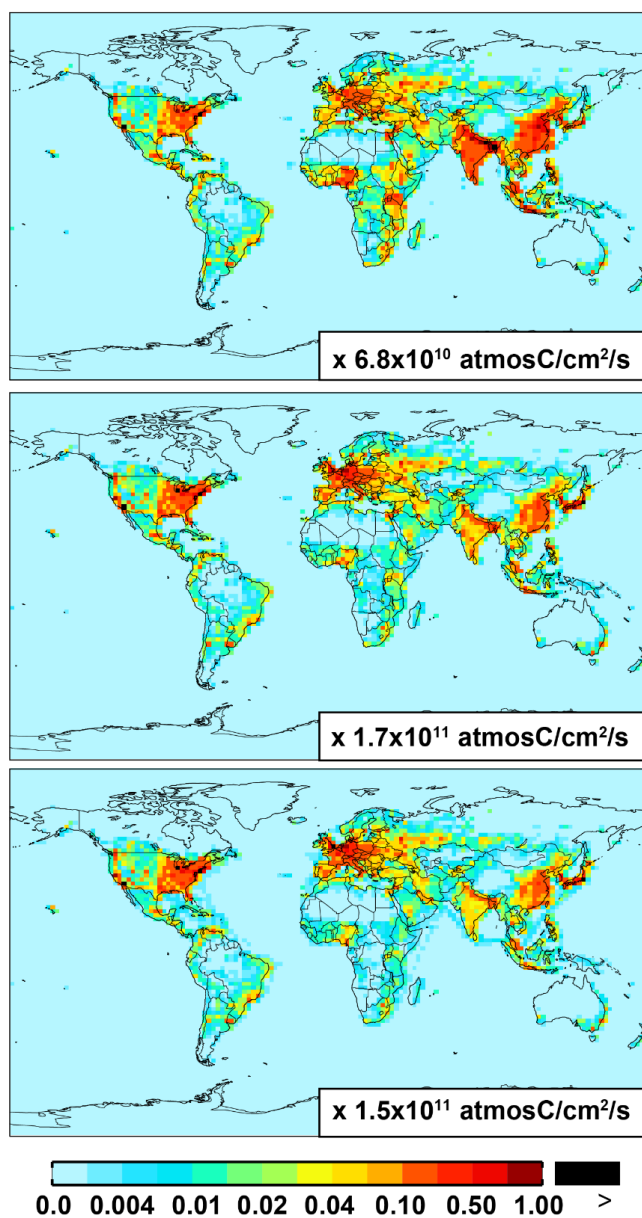


- 1 (EMEP) and observed atmospheric composition change during 1972-2009, *Atmospheric*
2 *Chemistry and Physics*, 12, 5447-5481, 10.5194/acp-12-5447-2012, 2012.
- 3 van der Werf, G. R., Randerson, J. T., Giglio, L., Collatz, G. J., Mu, M., Kasibhatla, P. S.,
4 Morton, D. C., DeFries, R. S., Jin, Y., and van Leeuwen, T. T.: Global fire emissions and the
5 contribution of deforestation, savanna, forest, agricultural, and peat fires (1997-2009),
6 *Atmospheric Chemistry and Physics*, 10, 11707-11735, 10.5194/acp-10-11707-2010, 2010.
- 7 Wesely, M. L.: PARAMETERIZATION OF SURFACE RESISTANCES TO GASEOUS DRY
8 DEPOSITION IN REGIONAL-SCALE NUMERICAL-MODELS, *Atmospheric Environment*,
9 23, 1293-1304, 10.1016/0004-6981(89)90153-4, 1989.
- 10 Yan, Y., Lin, J., Chen, J., and Hu, L.: Improved simulation of tropospheric ozone by a global-
11 multi-regional two-way coupling model system, *Atmospheric Chemistry and Physics*, 16, 2381-
12 2400, 10.5194/acp-16-2381-2016, 2016.
- 13 Yan, Y. Y., Lin, J. T., Kuang, Y., Yang, D., and Zhang, L.: Tropospheric carbon monoxide over
14 the Pacific during HIPPO: two-way coupled simulation of GEOS-Chem and its multiple nested
15 models, *Atmospheric Chemistry and Physics*, 14, 12649-12663, 10.5194/acp-14-12649-2014,
16 2014.
- 17 Yan, Y., Lin, J., and He, C.: Ozone trends over the United States at different times of day, *Atmos.*
18 *Chem. Phys.*, 18, 1185-1202, <https://doi.org/10.5194/acp-18-1185-2018>, 2018a.
- 19 Yan, Y., Pozzer, A., Ojha, N., Lin, J., and Lelieveld, J.: Analysis of European ozone trends in the
20 period 1995–2014, *Atmos. Chem. Phys.*, 18, 5589-5605, [https://doi.org/10.5194/acp-18-5589-](https://doi.org/10.5194/acp-18-5589-2018)
21 2018, 2018b.
- 22 You, X. Q., Senthilselvan, A., Cherry, N. M., Kim, H. M., and Burstyn, I.: Determinants of
23 airborne concentrations of volatile organic compounds in rural areas of Western Canada, *Journal*
24 *of Exposure Science and Environmental Epidemiology*, 18, 117-128, 10.1038/sj.jes.7500556,
25 2008.
- 26 Zhang, L., Jacob, D. J., Yue, X., Downey, N. V., Wood, D. A., and Blewitt, D.: Sources
27 contributing to background surface ozone in the US Intermountain West, *Atmospheric Chemistry*
28 *and Physics*, 14, 5295-5309, 10.5194/acp-14-5295-2014, 2014.
- 29 Zhang, Y. Z., and Wang, Y. H.: Climate-driven ground-level ozone extreme in the fall over the
30 Southeast United States, *Proceedings of the National Academy of Sciences of the United States*
31 *of America*, 113, 10025-10030, 10.1073/pnas.1602563113, 2016.

32



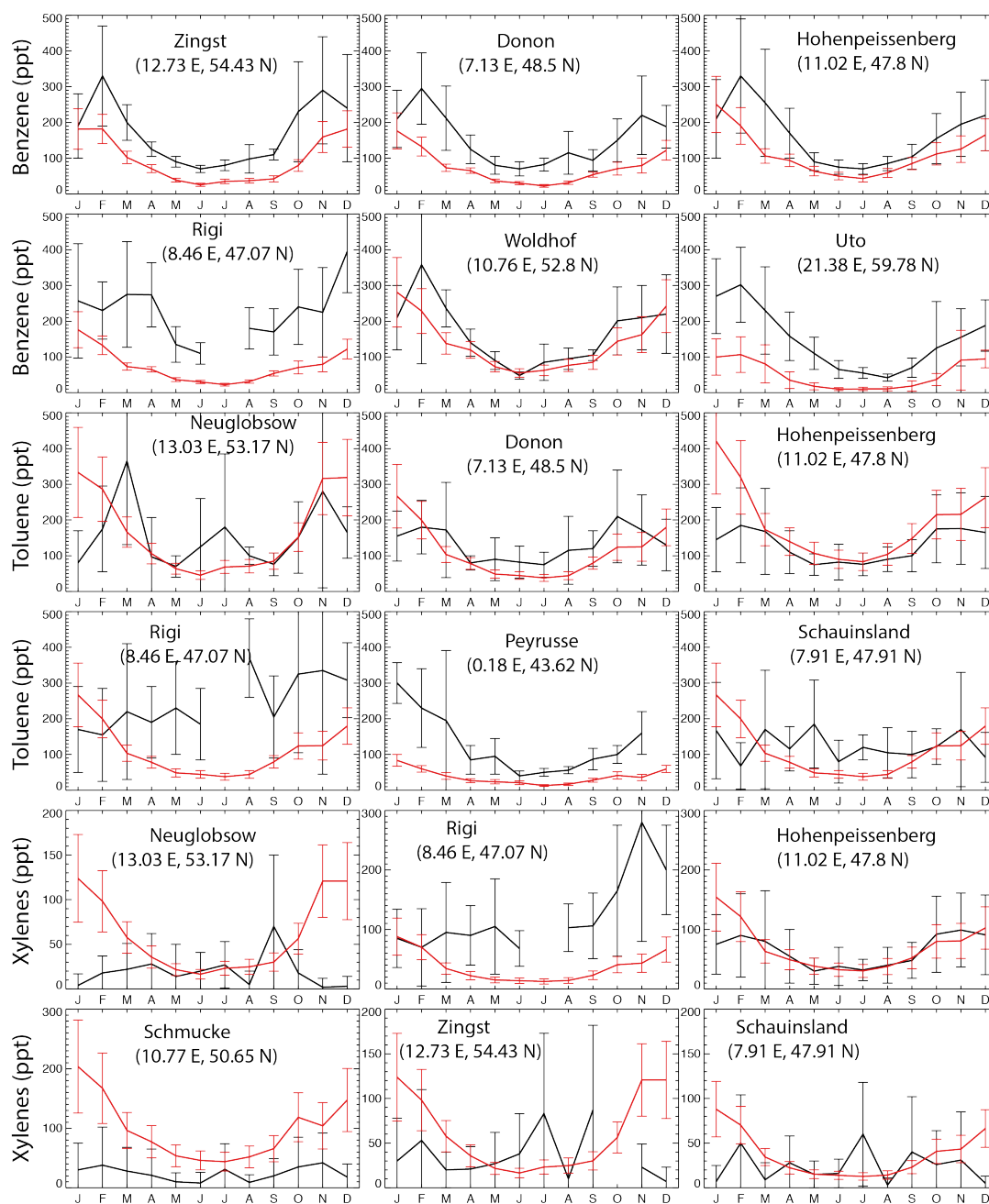
1



2

3 Figure 1. Spatial distribution of anthropogenic emissions from RETRO for benzene (top), toluene
4 (middle), and xylenes (bottom), respectively.

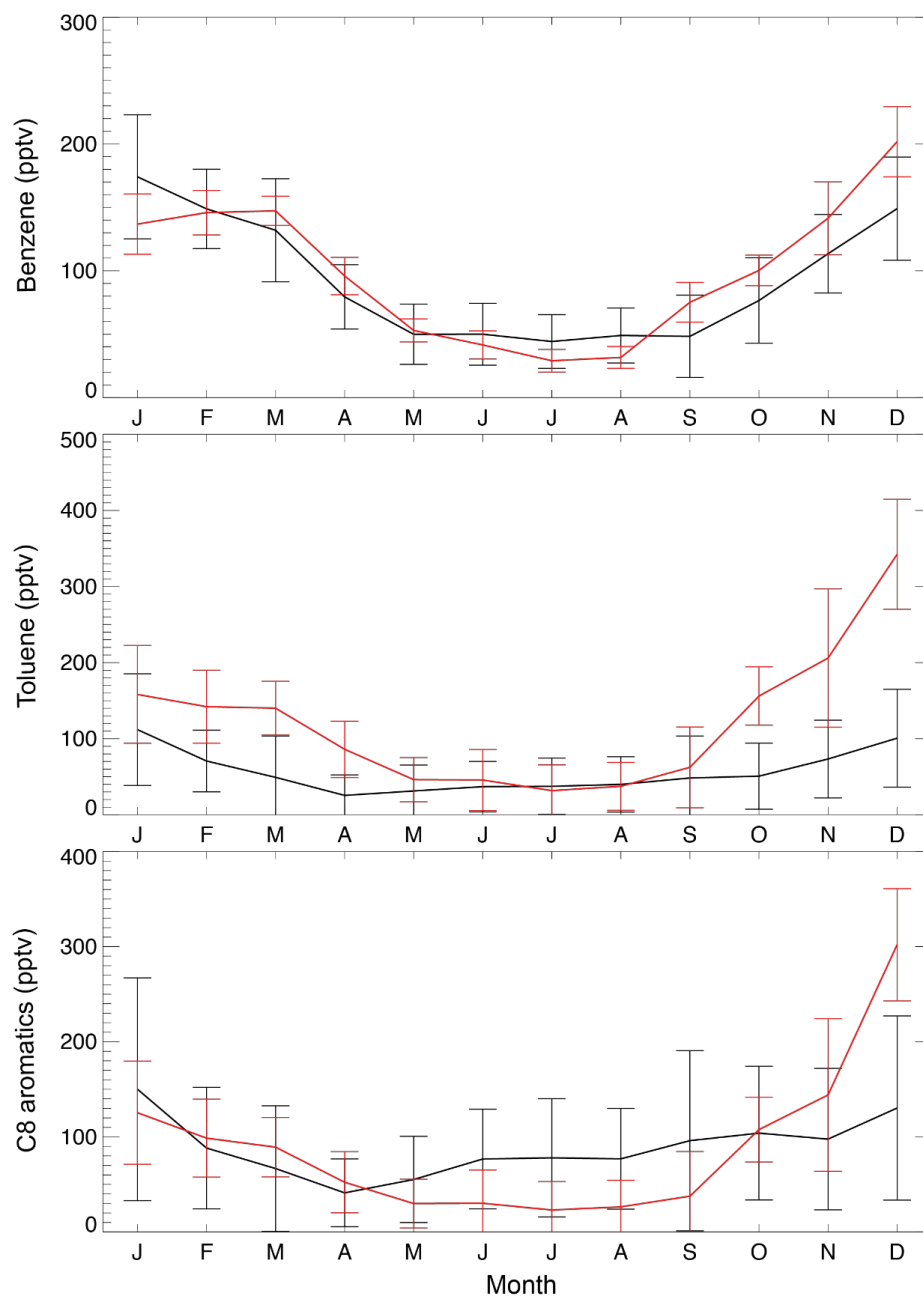
5



1

2 Figure 2. Monthly average EMEP observations (in black) of benzene (first two rows), toluene (middle two
3 rows) and xylenes (last two rows) at six different locations for the year 2005, as well as the model results
4 in the SAPRC simulation (in red), both in ppt. Error bars show the standard deviations.

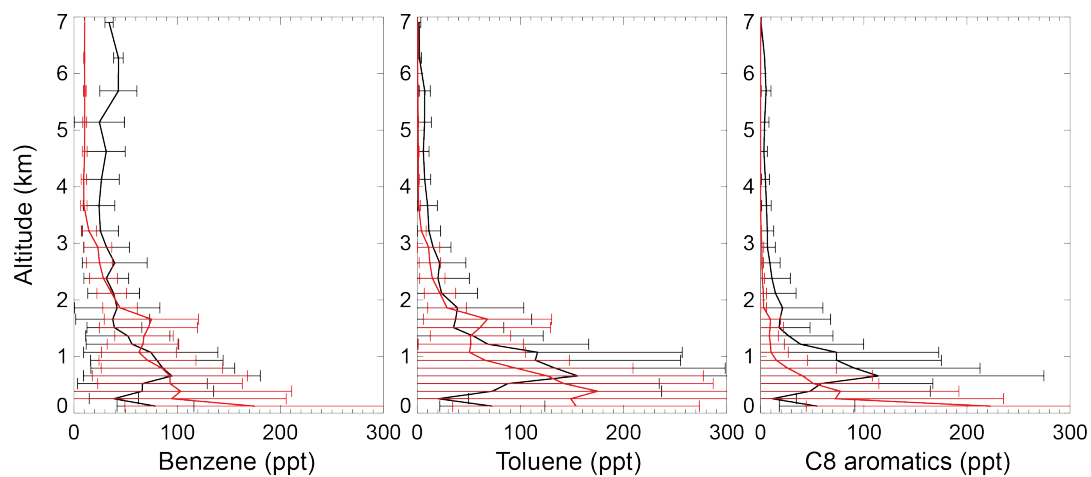
5



1

2 Figure 3. Monthly average KCMP tall tower observations (in black) of benzene, toluene and C₈ (xylenes +
3 ethylbenzene) aromatics in the year 2011 and the model results in the SAPRC simulation (in red). Error
4 bars show the standard deviations.

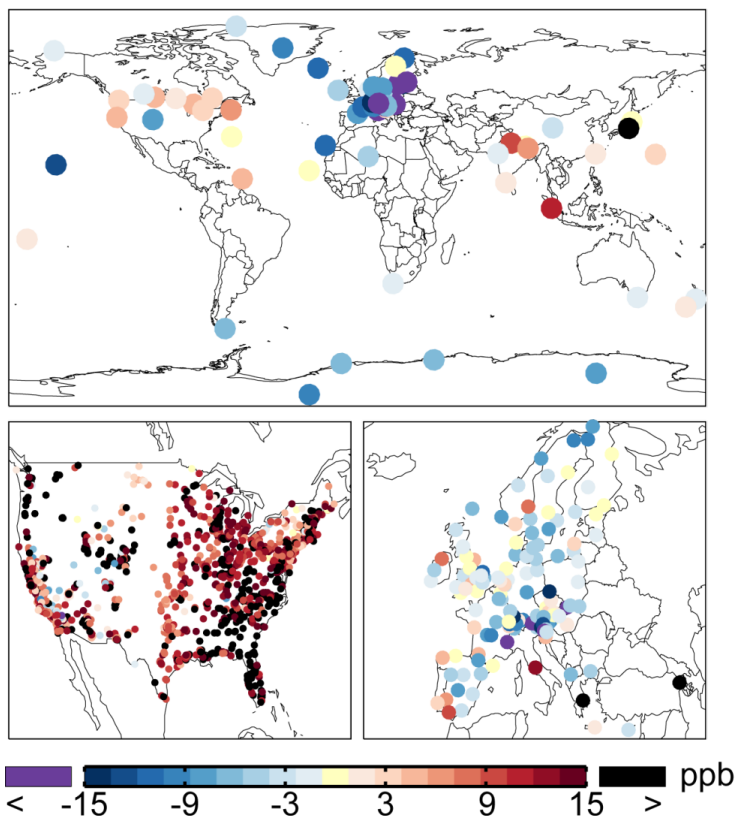
5



1

2 Figure 4. Measured (black) and simulated (red for the SAPRC case) vertical profiles of aromatics in
3 May/June 2010 for the CALNEX campaigns. Model results are sampled at times and locations
4 coincident to the measurements. Horizontal lines indicate the standard deviations.

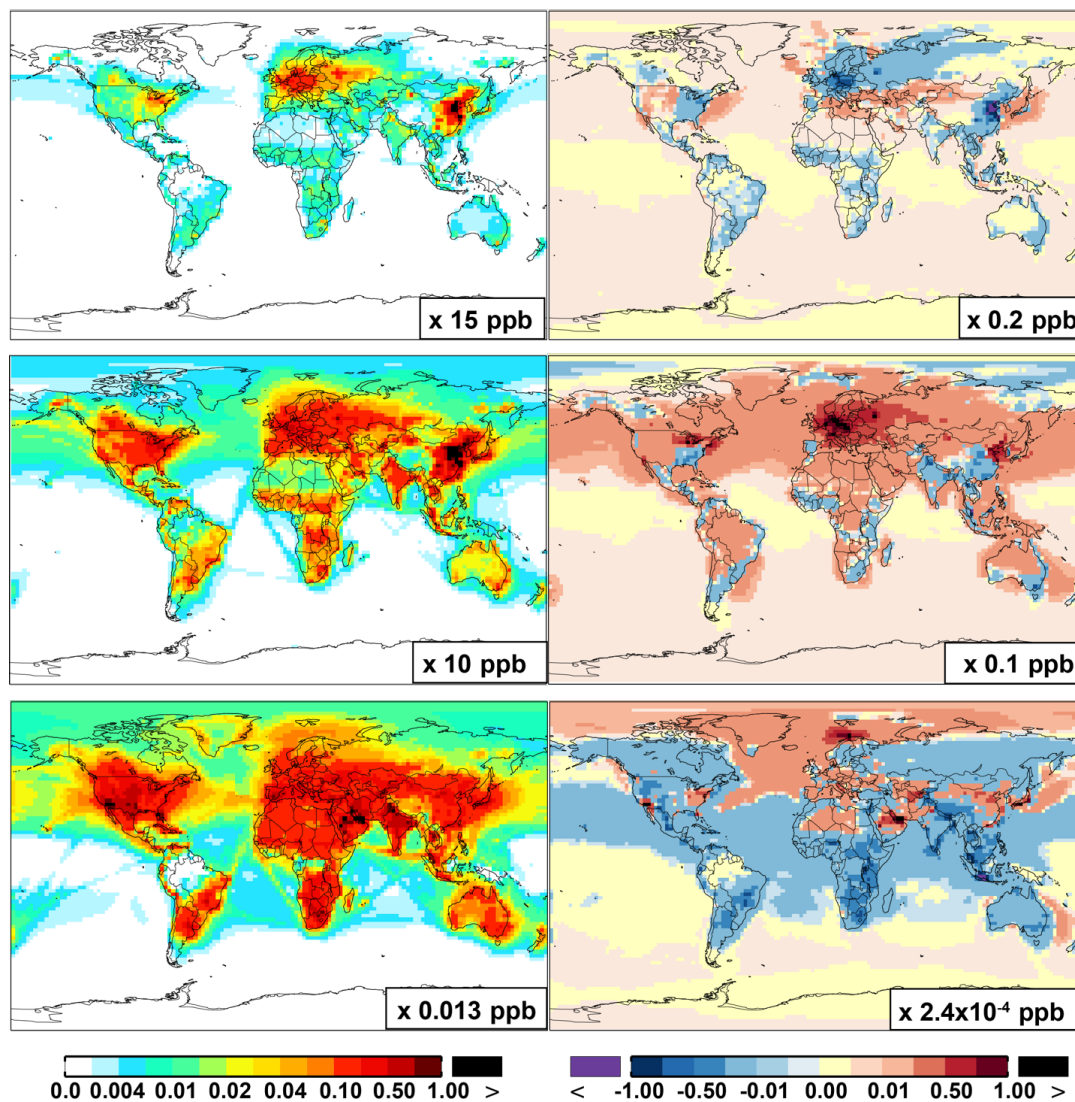
5



1

2 Figure 5. Annual mean model biases for surface ozone in the SAPRC simulation, with respect to
3 measurements from WDCGG (top panel), AQS (bottom left panel) and EMEP (bottom right panel)
4 networks.

5

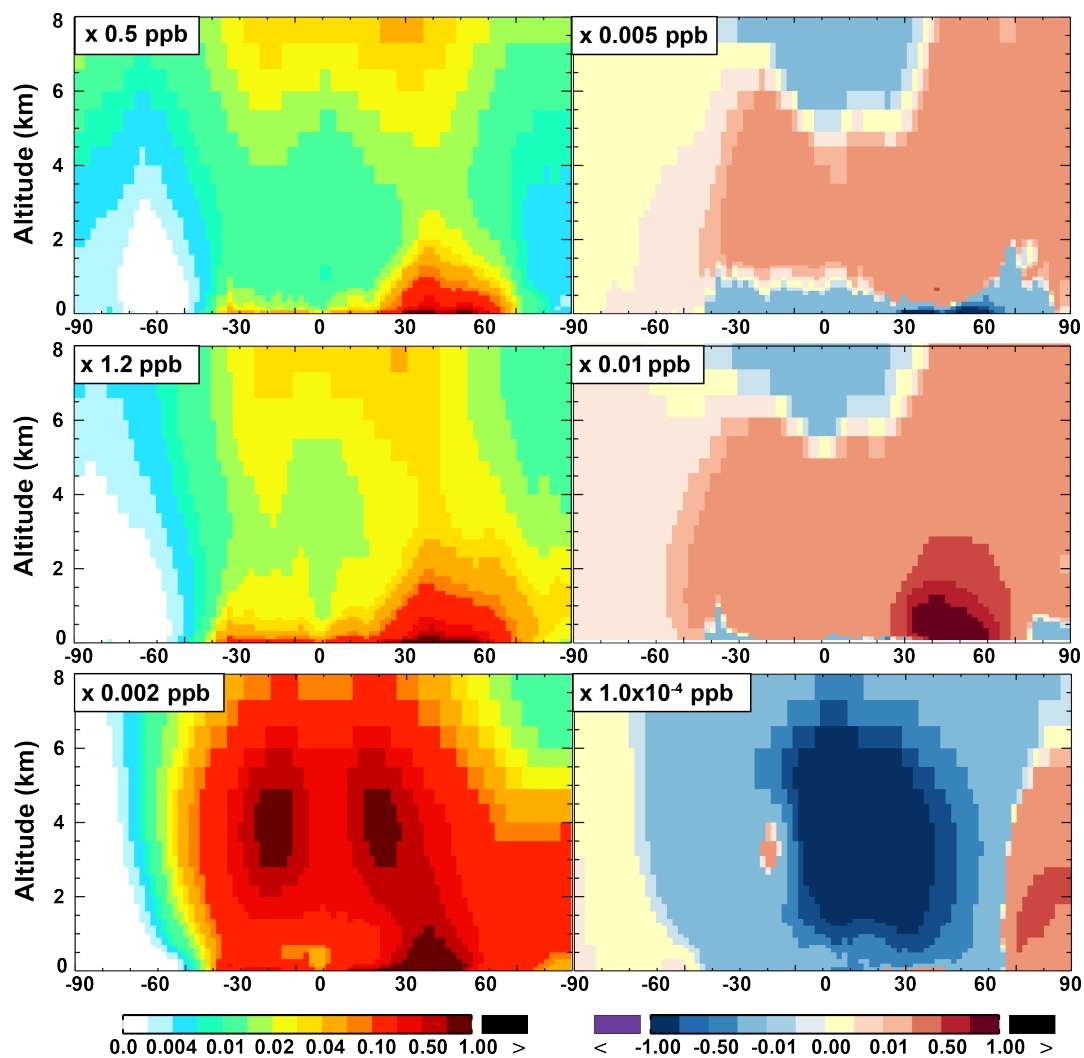


1
 2
 3
 4

Figure 6. (Left column) Modeled spatial distributions of surface NO (top), NO₂ (middle), and NO₃ (bottom) simulated in the Base case. (Right column) The respective changes from Base to SAPRC.



1



2

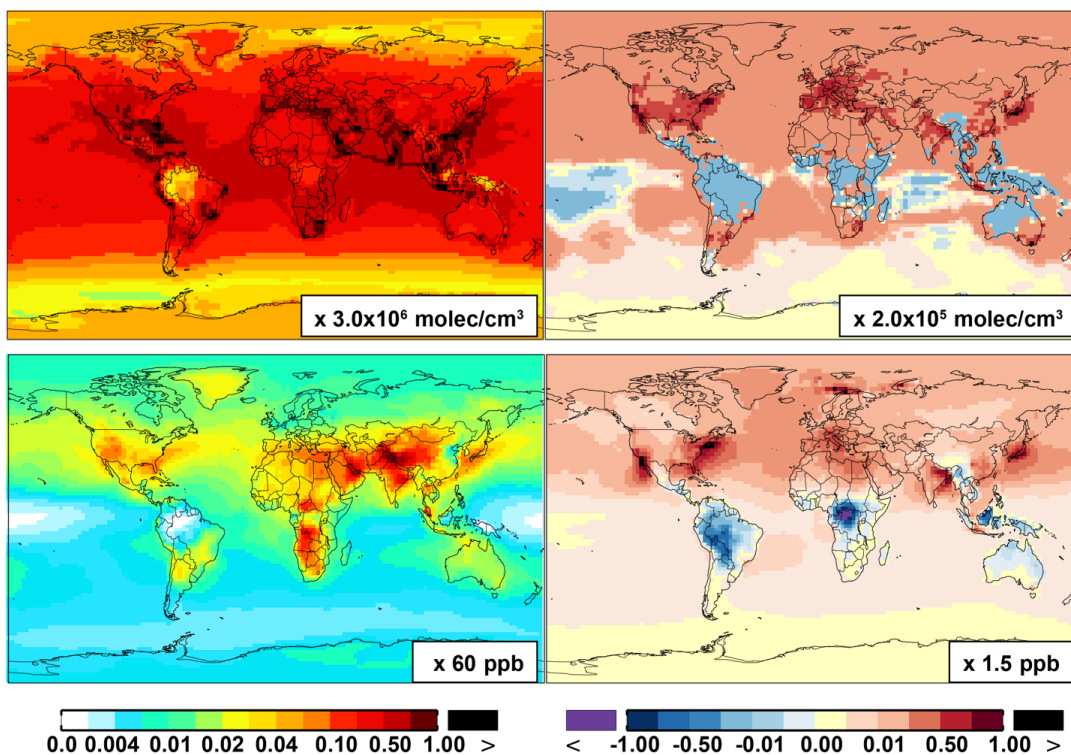
3 Figure 7. (Left column) Modeled zonal average latitude-altitude distributions of NO (top) and NO₂
4 (bottom) simulated in the Base scenario. (Right column) The respective changes from Base to SAPRC.

5

6



1



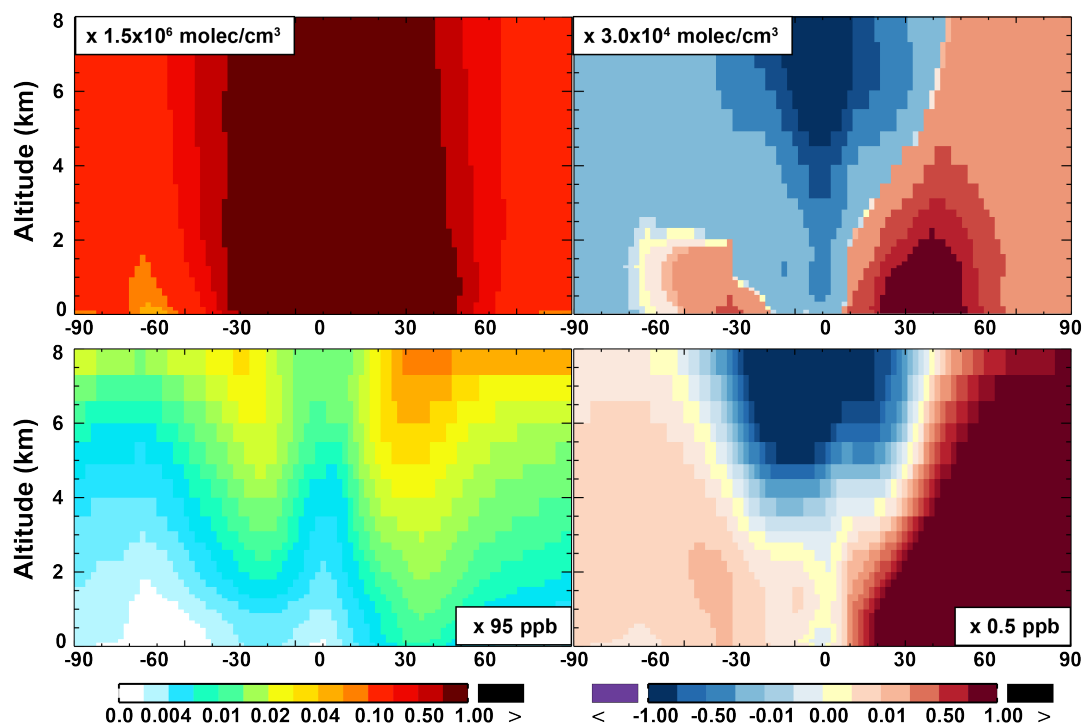
2

3 Figure 8. Same as Fig. 6 but for OH (top panels) and O₃ (bottom panels).

4



1



2

3 Figure 9. Same as Fig. 7 but for OH (top panels) and O_3 (bottom panels).

4

5



- 1 Table 1. Summary of the statistical comparison between observed and simulated concentrations (ppt for
- 2 aromatics, ppb for ozone). MMOD and MOBS represent the mean values for the SAPRC simulation and
- 3 the observation, respectively. SMOD and SOBS are their standard deviations. TCOR and SCOR are the
- 4 temporal and spatial correlations between model results and measurements.

Species	Network	Number of locations	Time resolution	MMOD	MOBS	SMOD	SOBS	TCOR	SCOR
Benzene	CARIBIC	1241	Instantaneous	12.3	16.0	4.2	15.8	-	0.31
	EEA	22	Annual mean	131.6	194.0	32.1	118.4	-	0.49
	EMEP	14	Monthly	106.5	166.4	38.7	71.7	0.77	0.44
	CALNEX	7708	Instantaneous	66.1	57.7	78.3	57.7	-	0.51
	KCMP	1	Hourly	99.9	91.5	92.6	56.7	0.65	-
Toluene	CARIBIC	789	Instantaneous	1.5	3.6	0.7	7.5	-	0.36
	EEA	6	Annual mean	180.9	240.3	66.8	59.4	-	0.41
	EMEP	12	Monthly	113.2	133.1	47.3	66.2	0.81	0.47
	CALNEX	7708	Instantaneous	80.6	73.2	179.7	131.9	-	0.46
	KCMP	1	Hourly	121.2	56.7	191.4	54.7	0.51	-
Xylenes	EMEP	8	Monthly	78.4	42.3	34.5	41.9	0.78	0.48
C ₈ aromatics	CALNEX	7708	Instantaneous	28.8	48.6	112.2	97.2	-	0.39
	KCMP	1	Hourly	88.9	90.3	119.2	79.5	0.46	-
Ozone	WDCGG	64	Monthly	28.6	34.1	12.8	14.2	0.68	0.54
	AQS	1214	Monthly	36.3	24.2	10.2	13.1	0.92	0.43
	EMEP	130	Monthly	27.7	30.6	13.2	10.3	0.76	0.52

5

6



1 Table 2. Annual and seasonal mean changes (%) in modeled surface as well as tropospheric
2 concentrations from the Base to the SAPRC simulation.

Species	Annual		MAM		JJA		SON		DJF	
	Surface	Trop								
NO	-0.2%	0.6%	-0.4%	0.7%	-1.3%	-0.1%	-1.5%	-0.5%	0.8%	1.6%
O ₃	0.9%	0.4%	1.1%	0.5%	0.6%	0.3%	0.8%	0.4%	1.0%	0.4%
CO	0.8%	1.0%	0.5%	0.7%	1.1%	1.2%	1.1%	1.3%	0.5%	0.7%
HNO ₃	1.1%	0.3%	1.2%	0.4%	0.7%	-0.1%	1.0%	0.2%	1.4%	0.6%
H ₂ O ₂	2.6%	1.5%	2.4%	1.5%	2.8%	1.5%	2.9%	1.7%	2.4%	1.4%
N ₂ O ₅	2.0%	2.1%	0.8%	-2.6%	-0.3%	-3.7%	1.4%	0.4%	3.1%	4.7%
NO ₂	1.0%	2.1%	0.8%	1.8%	-0.2%	0.6%	0.5%	1.3%	2.0%	3.6%
NO ₃	-0.9%	-4.1%	-1.5%	-5.6%	-0.9%	-3.7%	-0.5%	-3.4%	-0.8%	-4.1%
BENZ	-0.5%	-0.4%	-0.9%	-1.0%	0.1%	0.7%	-0.1%	0.2%	-0.6%	-0.6%
TOLU	-1.2%	-1.9%	-1.5%	-2.8%	-0.8%	-0.9%	-1.0%	-1.5%	-1.3%	-1.9%
XYLE	-1.4%	-2.3%	-1.2%	-2.1%	-1.2%	-1.5%	-1.6%	-2.3%	-1.5%	-2.4%
OH	1.1%	0.2%	1.4%	0.4%	1.2%	0.3%	0.9%	0.1%	1.0%	0.1%
HO ₂	3.0%	1.3%	2.9%	1.4%	3.3%	1.3%	3.1%	1.3%	2.8%	1.2%

3

4



1 Table 3. Annual and seasonal mean model ozone biases for the Base and the SAPRC case, compared to
 2 measurements from WDCGG, AQS and EMEP.

Species (ppb)	Annual		MAM		JJA		SON		DJF	
	Base	SAPRC	Base	SAPRC	Base	SAPRC	Base	SAPRC	Base	SAPRC
WDCGG	-6.0	-5.4	-9.0	-8.4	-0.4	0.1	-2.5	-2.1	-11.9	-11.5
EMEP	-3.5	-2.8	-5.5	-4.7	4.5	5.2	0.3	0.8	-13.1	-12.8
AQS	11.4	12.0	7.3	8.1	13.7	14.3	12.1	13.0	12.3	12.9

3

4

5

6